

Detecting Robust Patterns in the Spread of Epidemics: A Case Study of Influenza in the United States and France

Pascal Crépey^{1,2} and Marc Barthélemy^{3,4}

¹*Unité 707, Institut national de la Santé et de la Recherche médicale, Paris, France*

²*Unité mixte de Recherche en Santé 707, Université Pierre et Marie Curie,*

Faculté de Médecine Pierre et Marie Curie, Paris, France

³*Centre d'Etudes de Bruyères-le-Châtel, DAM Ile-de-France,*

Commissariat à l'énergie atomique, Bruyères-Le-Châtel, France

⁴*School of Informatics and Center for Biocomplexity, Indiana University, Bloomington, IN*

(Dated: October 29, 2018)

In this paper, the authors develop a method of detecting correlations between epidemic patterns in different regions that are due to human movement and introduce a null model in which the travel-induced correlations are cancelled. They apply this method to the well-documented cases of seasonal influenza outbreaks in the United States and France. In the United States (using data for 1972-2002), the authors observed strong short-range correlations between several states and their immediate neighbors, as well as robust long-range spreading patterns resulting from large domestic air-traffic flows. The stability of these results over time allowed the authors to draw conclusions about the possible impact of travel restrictions on epidemic spread. The authors also applied this method to the case of France (1984-2004) and found that on the regional scale, there was no transportation mode that clearly dominated disease spread. The simplicity and robustness of this method suggest that it could be a useful tool for detecting transmission channels in the spread of epidemics.

PACS numbers: 89.75.Hc, 87.23.Ge, 87.19.Xx

Understanding quantitatively how a disease spreads in modern society is a crucial issue. In particular, the high probability of occurrence of the next influenza pandemic raises interest in the design of efficient containment policies [1, 2, 3, 4, 5] and necessitates an accurate characterization of spatiotemporal epidemic patterns. Recent outbreaks of highly communicable diseases [6, 7, 8, 9, 10, 11] have triggered a series of studies on the mechanisms of global disease spread [5, 12, 13, 14], and other studies have addressed the issue at the level of individual countries [1, 2, 15, 16]. In all of these studies, the travel and movement of individuals is a crucial point [5, 12, 14, 16, 17, 18, 19]. It is of the highest importance for control strategies to identify the main channels of transmission or "epidemic pathways", if any [14]. Indeed, identifying such pathways provides a first hint on how to control a disease's spread. Even if, in most cases, travel restrictions are economically unrealistic, knowing the most important transmission channels could help to slow down the epidemic through the use of selective travel restrictions. In addition to epidemics of emergent diseases, recurrent influenza epidemics are a burden for societies located in temperate areas. They affect approximately 5-15 percent of the population worldwide and are responsible for 250,000-500,000 deaths annually [20]. Different influenza surveillance systems have been set up in various parts of the world [21, 22, 23], and influenza has been tracked for a long time (the World Health Organization Global Influenza Surveillance Network was established in 1952), which makes it a well-documented disease. These data provide an important ground for testing and developing strategies and for uncovering the main transmission mechanisms of a disease at different scales. Indeed, the spread of influenza has been the focus of many studies for several years, and a number of models have been proposed to describe and understand it [17, 24, 25, 26, 27]. Other in-

vestigators have thoroughly described the spatial distribution of influenza spread [28, 29] and of annual waves of infection in the United States [15, 16]. Because of the complexity of epidemic processes, together with the "noise" present in data, innovative statistical analyses need to be developed for detecting patterns. For example, using signal processing methods, Brownstein et al. [16] recently found evidence of correlations between domestic airline volume and the transnational spreading time of influenza. We think that at this point the convergence of different methods is critical, and in this paper we propose another method which requires little data manipulation and filtering. In this paper, we discuss our results in the light of recent studies [15, 16] and bring our perspective to issues such as the existence of preferred channels of transmission and the impact of travel restrictions. We have developed a robust and relatively simple method of detecting correlations between different areas—"robust spatial patterns"—in empirical data on disease dynamics. In this paper, we illustrate and apply this method to the well documented cases of influenza dynamics in the United States and France. Our goal was to detect genuine correlations between different regions and to use as few assumptions as possible. The problem originates in the fact that a correlation coefficient usually aggregates different phenomena. In addition, large correlation coefficients can arise from external large-scale environmental constraints but do not reflect the existence of actual correlations due to other factors such as human movements. In order to characterize the level of correlation in a particular system under study, we need a reference (or "null") model which gives us the corresponding value of the correlation coefficient in the absence of transportation flows. In this paper, we propose a method of obtaining such a null model and apply it to the dynamics of influenza transmission in the United States and France. In both cases, we find robust transmission channels for epidemic

spread. In a second step, we try to relate the existence of such channels to transportation flows.

I. MATERIAL AND METHODS

A. Data sets

We analyzed interpandemic influenza epidemics occurring during the periods 1972-2002 for the United States and 1984-2004 for France. In both cases, we defined an influenza "epidemic period" as a year running from September to September, in order not to truncate the epidemic season. For the United States, we used weekly state-specific mortality rates for pneumonia and influenza collected by the Centers for Disease Control and Prevention, restricted to the 48 contiguous states and the District of Columbia. According to Viboud et al. [15] and Greene et al. [28], the weekly time series of pneumonia and influenza mortality appear to be useful indicators of the time evolution of spatial spread and, interpreted cautiously, incidence within each state. For France, we used estimates of the daily incidence of influenza-like illness in each region, and we restricted our study to the 21 continental regions of France. Those estimates were based on data collected by the Sentinel Network [21], a network of general practitioners distributed throughout the entire French territory. The estimates were in agreement with drug-sales data, which confirms their relevance [30]. We investigated a possible relation between our indicator and several types of transportation flow. Data on yearly air traffic and commuter volumes in the United States, by state, were obtained from the Bureau of Transportation Statistics (unpublished data; <http://www.bts.gov>) and the Census Bureau [31]. Data on French interregional train-traffic volume per year were obtained from the French National Railway Service (unpublished data; <http://www.sncf.fr>), and interregional automobile traffic volume was based on 2001 data obtained from the Service d'Etudes techniques des Routes et Autoroutes (unpublished data; <http://www.setra.equipement.gouv.fr>). We also took into account geographic distances between states or regions, approximated by using the distances between state capitals for the United States and the distances between regional prefectures for France. To investigate the possible effect of climate, we used weekly temperature data for US states for the period 1995-2006, obtained from the National Weather Service [32].

B. Methods

We investigated separately in the two data sets a correlation coefficient-based indicator which enabled us to assess the importance of travel flows. For the United States, results were computed over 30 years of weekly data, and for France they were computed over 20 years of daily data. For all pairs of areas i and j , we computed the usual Pearson correlation coefficient r_{ij} for incidence over each epidemic period (see Appendix). The value of this coefficient is usually difficult to interpret, however, and needs a comparison value. Thus, we

propose below a simple way to cancel correlations in real data (uncorrelated model). We also estimate the maximal correlation that one can observe in the system under study. These values, obtained for the uncorrelated and maximally correlated models, define an interval which allows for a quantitative estimate of the correlations existing between different areas.

Uncorrelated model. If the spread of a disease in a country is essentially due to the travel of infected persons between cities, there will be a particular time ordering of the activity profiles for different areas. The extreme case corresponds to carriers who can make only short-range displacements, leading to a spatial diffusion phenomenon with a well-defined epidemic front propagating at a given velocity (which was the case, for example, for the Black Death [33, 34]). In this case, an outbreak appears at a time that is directly related to the distance from the initial infectious seed. In modern societies, people can travel over large distances, which dramatically modifies the spatial diffusion of the disease and its simple propagating front; however, there should still be a pattern. Indeed, if an infected person carries the disease from an infected area A to a noninfected area B and transmits the disease in area B , we will observe a time difference between the epidemic peaks in the two areas. We can expect that the larger the flow between areas A and B , the greater the similarity between the epidemic profiles in the two areas. The time ordering and the correlation between the epidemic profiles in different regions is thus a signature of the flow of infected individuals. Unfortunately, epidemic activities usually occur over a short period of time in all regions of a country, and a large observed correlation could result from this short-period constraint without producing significant information about transmission channels. The aim of the natural null model is to eliminate the large correlation value occurring by chance. Therefore, it corresponds to a random time shift of the activity profiles of the different regions. If the values of the actual correlation coefficient are then significantly larger than the ones obtained with the null model corresponding to epidemics emerging at random times, it is the signature of genuine correlations induced by the displacement of individuals from one region to another. For every epidemic period (from September to September), we define the "epidemic activity time range", which contains all peaks for all regions or states. We then shift, by a random amount drawn from a uniform probability, the whole epidemic profile of a region or state, such that the epidemic profile still belongs to the epidemic activity time range (figure 1, parts A and B). The next step is to compute the Pearson correlation coefficients for all pairs of areas—for a given year—and for a large number of random shifts. We finally obtain the average correlation coefficient m_{ij} between all pairs of areas i and j for the uncorrelated (or "null") model.

Maximal correlation. The correlation between two areas will be maximal for very similar "synchronized" activity profiles with activity peaks reached essentially at the same time. In order to obtain this maximal value for the correlation coefficient for a given pair of areas and a given year, we compute the cross-correlation of the epidemic profiles of the two areas. When the maximum correlation coefficient is found, we

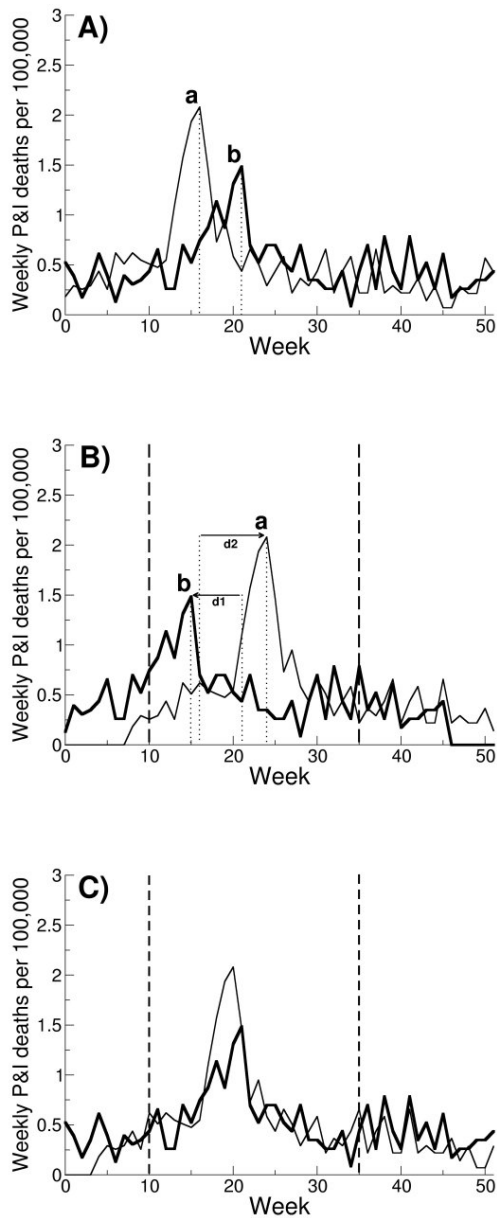


Figure 1: Model of maximal correlation and uncorrelated epidemic disease spread. A) Weekly rate of mortality from pneumonia and influenza (P&I) per 100,000 for two different US states. The letters a and b and the dotted lines indicate the corresponding epidemic peaks. B) Random reassignment of the peak moments, resulting in a shift of the different epidemic profiles by randomly chosen amounts d_1 and d_2 . C) The specific shift that gives the highest correlation coefficient for the pair of epidemic peaks and corresponds to a synchronization of the peaks. For parts B and C, the dashed lines indicate the "epidemic activity time range."

store it and reapply the method to the next pair of areas. Parts A and C of figure 1 illustrate the method and show epidemic

profiles with the shift that produces the maximum correlation coefficient (corresponding to epidemic peak synchronization as expected). The output is a matrix M_{ij} of maximal possible correlation coefficients for the pair of areas (i, j) for a given year.

A correlation coefficient-based indicator. The uncorrelated model gives the value of the correlation coefficient in the absence of time correlations in the peak value of the epidemic period, while the maximal value is obtained when the peaks are synchronized. We can combine these different values in order to obtain a parameter $X_{ij}(t)$ between areas i and j for year t :

$$X_{ij}(t) = \frac{r_{ij}(t) - m_{ij}(t)}{M_{ij} - m_{ij}(t)},$$

where we recall that r_{ij} , $m_{ij}(t)$, and $M_{ij}(t)$ denote the correlation coefficients obtained previously (calculated for year t). The coefficient X is thus bounded by 1 by construction, and since time reshuffling cancels essentially time-ordering correlations, poorly correlated and anticorrelated states can exist and have $r_{ij} < m_{ij}$, leading to negative values of X . Those values can even be very low when $M_{ij} - m_{ij} \ll 1$. Below, we analyze these quantities X for every year.

Robust patterns. We are looking for spatial patterns due to persistent factors which do not vary significantly from one year to another. We are thus interested in pairs of areas showing both a high value of X_{ij} and a low dispersion around this average, which indicates a regularity in the large values of X and hence a robustness in the bond between the corresponding areas. As we will see, most links have a relatively large average value $\langle X \rangle$, and the low level of fluctuation is simply characterized by the inverse coefficient of variation (CV) of X_{ij} , defined as

$$CV(X_{ij}) = \frac{\sqrt{\langle X_{ij}(t)^2 \rangle - \langle X_{ij}(t) \rangle^2}}{\langle X_{ij}(t) \rangle}.$$

A low standard deviation will then be associated with a high value of $1/CV(X_{ij})$.

Spatial autocorrelation. In order to determine the presence of spatial correlations in our indicator, we use Moran's I , which is a weighted correlation coefficient for X where the weights depend on the distance h between two regions. In our results we use binary weights, where 1 is attributed to pairs of states at a distance between h and $h + a$ and 0 otherwise.

II. RESULTS

In figure 2, we provide an example of average values of X over the period 1972–2002 between California and other US states. As we can see, most connections have a large average correlation, and the main point of interest in figure 2 concerns the heterogeneity of confidence intervals, which give information about the stability of the bond between two areas from year to year. Indeed, one can observe that some bonds have a highly fluctuating correlation (for Wisconsin, 95 percent confidence interval: 0.46, 0.92), while others display a remark-

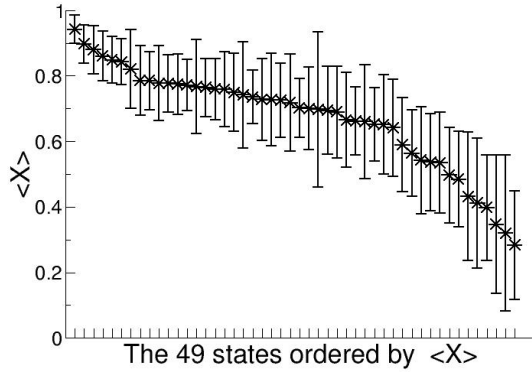


Figure 2: Average correlations of epidemic profiles between California (y-axis) and the other 48 US states (47 contiguous states plus the District of Columbia) (x-axis), computed for 30 epidemic periods (1972–2002). Data are ranked from the highest value to the lowest. Bars, 95% confidence interval.

able robustness (for Arizona, 95 percent confidence interval: 0.84, 0.94), which is the signature of a stable recurring pattern.

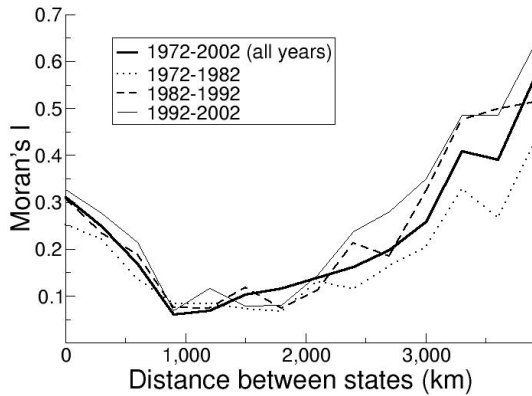


Figure 3: Spatial autocorrelation of X . The graph shows Moran's I computed over X , plotted as a function of the distance between states. Pairs of states are grouped by the distance between them, within a 300-km band. The bold line shows the evolution of the correlation measure for X averaged over 30 years (1972–2002). The thinner lines stand for X averaged over three different decades. The curves all display the same trends, showing stability of the spreading pattern over time.

We also must consider spatial autocorrelation analysis on the X indicator. We aggregate data for all of the states and show, in figure 3, the evolution of Moran's I with different threshold distances h . In the same plot, we show the results for

X averaged over all years in our data set (1972–2002) or averaged over three different decades. The spatial autocorrelation reveals correlation clusters at both short and long distances. Figure 3 also shows that our results are stable over time.

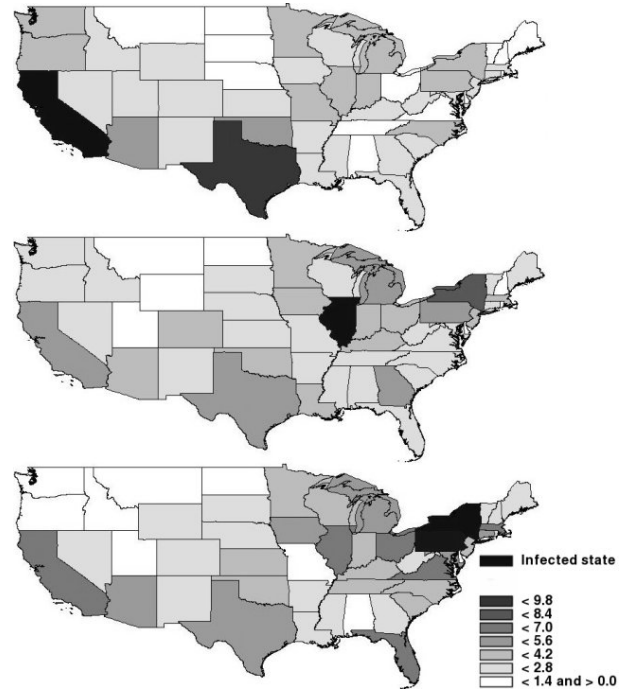


Figure 4: Correlations of epidemic profiles for three US states (denoted as "infected state"). The various shades of gray stand for values of $1/CV(X_{ij})$, where i corresponds to California, Illinois, or New York (top to bottom) and j to all of the other states. In each map, black stands for the considered state (California, Illinois, or New York). We observe high values of $1/CV(X_{ij})$ for neighboring states (Arizona for California; Indiana, Kentucky, and Ohio for Illinois; New Jersey, Pennsylvania, and Massachusetts for New York) and long-range connections between California and Texas, Illinois and New York, and New York and California.

Figure 4 displays the results for the correlation ($1/CV(X_{ij})$) on maps for three different states. In the three situations, we observe high $1/CV(X_{ij})$ values for neighboring states, as well as long-range bonds. This method can also be used on the smaller scale of French regions. We also observe two types of strong connections here (figure 5). Regions are strongly correlated with their neighbors, and we observe long-range strong connections, as in the case of the United States.

A. Relation with transportation data

In figures 6 and 7, we plot the quantity $1/CV(X)$ against transportation traffic data to test its relation to transportation flows. In figure 6, we plot $1/CV(X)$ against the interstate US air-traffic flow. The linear fit computed has a coefficient of de-

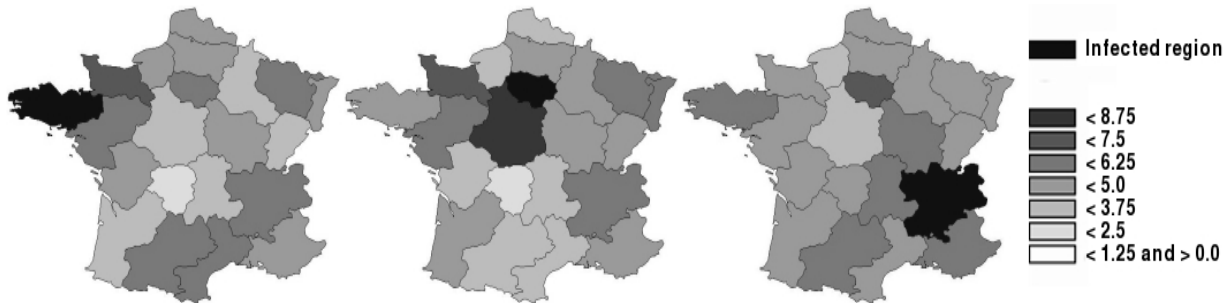


Figure 5: Correlations of epidemic profiles for three regions in France (denoted as "infected region"). The various shades of gray stand for values of $1/CV(X_{ij})$, where i corresponds to Bretagne, Ile-de-France, or Rhone-Alpes (left to right) and j to all of the other regions. In each map, black stands for the considered region (Bretagne, Ile-de-France, or Rhone-Alpes).

termination of 0.74 and thus supports evidence that $1/CV(X)$ is proportional to the air-traffic flow (note that we have not normalized the traffic with respect to the population). This plot supports the claim that $1/CV(X)$ indicates that the main vector for the spread of an epidemic in the United States is domestic air traffic. In order to assess the specific contribution to our indicator of air traffic as compared with other parameters, such as temperature or geographic distance, we performed a multivariate regression analysis using a linear model. For temperature, we used the Pearson correlations of weekly reported temperatures between states. We used state temperature profiles covering 11 years to control for possible artifacts. The results of this analysis (table II A) suggest that interstate air traffic makes a greater contribution than distance or temperature (estimates were 0.407, 0.096, and 0.220, respectively). Although the model does not explain the total variance ($r^2 = 0.27$), it is statistically significant ($p < 0.001$) and suggests that air travel is the dominant factor among those factors explored.

As recent studies have shown [15, 35], travel to work [31] plays a predominant role in disease spread, and thus we estimated its impact on our results. The volume of interstate commuting is very low (representing approximately 3 percent of the total number of US commuters) and decreases quickly with distance, so we needed to consider only pairs of states with common borders. Through a multivariate regression on $1/CV(X)$, we compared the impacts on epidemic spread of air travel and commuting using ground modes of transportation. Air traffic made a larger contribution in the regression model (table III), and we can thus conclude that it is the dominant transportation mode, even between neighboring states. On a smaller scale, the results for France were more contrasted. As figure 7 shows, the behavior of $1/CV(X)$ increased with train traffic, but we also performed a linear multivariate regression analysis of $1/CV(X)$ as a function of train traffic, automobile traffic, and geographic distance. Our aim was not to obtain a fully explicative model but to test whether one of these factors would dominate the others. The results (table III) show that distance makes little contribution to the model and that automobile and train traffic have essentially

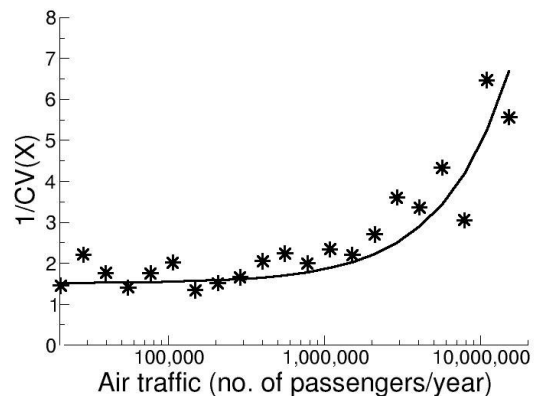


Figure 6: Correlation indicator for air transportation flow in the United States. The graph shows the inverse coefficient of variation (CV) of X as a function of domestic air transportation flow for all pairs of states (binned data). Since the range of variation of the traffic was very wide, the log-linear plot is shown. Air transportation was measured as the number of passengers traveling by plane between pairs of states in 2000. The curve is a linear fit of the equation $1/CV(X) = A * flow + B$, where $A = 2.5 * 10^{-7}$ and $B = 0.91$ ($r^2 = 0.74$).

the same weights (0.092, 0.265, and 0.204, respectively). As in the US case, the model does not explain all of the variance ($r^2 = 0.22$), but the result is statistically significant ($p < 0.001$).

III. DISCUSSION

We have presented a method that aims to identify strongly connected areas from raw epidemic data. Our main goal is to identify preferred spatial paths—or epidemic pathways—for the spread of infectious diseases. If these paths exist, they

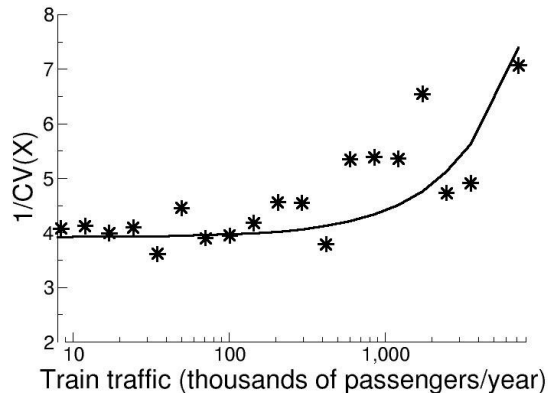


Figure 7: Correlation indicator for train traffic in France. The graph shows the inverse coefficient of variation (CV) of X as a function of train transportation for all pairs of regions (binned data). Since the range of variation of the traffic was very wide, the log-linear plot is shown. Train transportation was measured as thousands of passengers traveling by train between pairs of regions in 2001. The curve is a linear fit of the equation $1/CV(X) = A * flow + B$, where $A = 4.6 * 10^{-5}$, $B = 3.9$ ($r^2 = 0.52$).

	Estimate
Intercept	0
A: Air traffic volume	0.407
B: Distance between states	-0.096*
C: Temperature correlation	0.220*

* $p < 0.001$.

Table I: The linear regression equation takes the form $X = b_1 + b_2 * A + b_3 * B + b_4 * C$, where A , B , and C stand for standardized air traffic volume, distances between states, and correlation of state temperatures, respectively, and b_j are the estimates given in the table ($r^2 = 0.27$, $p < 0.001$).

have an effect on the spatiotemporal pattern of reported cases of disease; consequently, we should be able to identify them from the temporal evolution of local influenza incidence. An important fact is the need to discriminate what is due to inherent noise, spatial effects, and other constraints in the data. In order to achieve this goal, we define and use an uncorrelated model which cancels the existing correlations due to transportation flows. The maximal correlation gives the upper bound of the possible correlation that would exist between two areas if they were perfectly synchronized. These lower and upper bounds enable us to assess the level of genuine correlation due to transportation flow between regions. By observing data from several years, we can analyze the evolution of the level of correlation between areas and detect the robustness of patterns over time. The spatial autocorrelation analysis showed that the behavior of our indicator is stable over time. Results were consistent from one set of years to another, despite possible environmental evolution. This stability, particularly with

respect to the increase in air-travel flow (on the order of 300 percent between 1972 and 2002), seems to indicate that for some time now, air-travel flows have been large enough to propagate an epidemic throughout the United States. This implies that in order to be efficient, travel restrictions should be so drastic that they are economically unreasonable—a finding that agrees with other recent results [5, 15]. The spatial regression analysis also revealed the existence of geographic clusters of strongly correlated neighbor states at short distances (<600 km) and other clusters at long distances (>3,000 km). We cannot relate these results directly to the smaller scale (the intercounty level) studied by Viboud et al. [15], since we were using aggregated data, but as expected, our results were in agreement with those of that study at the larger interstate scale.

	Estimate
Intercept	0
A: Air traffic	0.341
B: Ground commuting	0.068

* $p < 0.001$.

Table II: The linear regression equation takes the form $X = b_1 + b_2 * A + b_3 * B + b_4 * C$, where A , B , and C stand for air traffic and commuting between states, respectively, and b_j are the estimates given in the table ($r^2 = 0.12$, $p < 0.001$).

The next step is to interpret these patterns in terms of social, geographic, or other epidemiologic data. In the case of the United States, we were able to relate the existence of persistent channels of transmission to interstate air transportation flows, while other factors such as climate seemed less important. We also showed that even between neighboring states, air travel is dominant over commuting using ground modes of transportation. Commuters very likely play a role in the spread of epidemics at the county level, and further investigation at this smaller scale is needed. More generally, such an interpretation might not be particularly feasible because of the mixing of different modes of transportation. Indeed, the case of France, which is of interest for its smaller scale, highlights the weakness of a hypothesis pertaining to a single mode of transportation. An explanation for this might be that different modes of travel (train, automobile, and plane) compete at this scale and there is no clearly dominant transportation mode, a result which is supported by our multivariate analysis. The existence of a large $1/CV(X)$, however, reveals the existence of strongly connected regions. The lack of clear correlations between large values of $1/CV(X)$ and large traffic volumes does not affect the quality of the indicator $1/CV(X)$ but simply reflects a more mixed situation concerning transportation modes used in the influenza epidemic process. There are different limitations to this work. In particular, pneumonia and influenza mortality (for the United States) or influenza-like illness (for France) are just proxies for laboratory-confirmed influenza. Moreover, we did not take into account the change in influenza strains from one year to another. However, these factors are unlikely to have affected our conclusions about robust transmission channels. Another possibly important limitation

concerns the fact that all studies (including ours) are limited to the spread of disease inside a given country and neglect the exchange of disease with other countries. The corresponding flows are usually far from negligible, and we think their importance in national spread should be assessed in future studies. Our heavy use of retrospective data to compensate

	Estimate
Intercept	0
A: Distance between regions	-0.092 \dagger
B: Automobile traffic volume	0.265*
C: Train traffic volume	0.204*

* $p < 0.001$, $\dagger p < 0.1$.

Table III: The linear regression equation takes the form $X = b_1 + b_2 * A + b_3 * B + b_4 * C$, where A , B , and C stand for standardized, distances between regions, automobile traffic volume, and train traffic volume, respectively, and b_j are the estimates given in the table ($r^2 = 0.22$, $p < 0.001$).

for data fluctuations did not allow us to analyze and interpret single-year fluctuation as shown in the paper by Brownstein et al. [16]. Basically, those authors chose a different trade-off than ours and decided to aggregate their data in a few US

geographic regions, whereas we decided to keep a statewide approach and use as many years as possible. Our results seem to suggest that for the United States, realistic modeling of the spread of epidemics at the interstate level may only need to take air transportation into account. They also seem to imply that in the case of France, a realistic model would need to include several transportation modes. In summary, we believe that this simple and robust method, which detects important channels of disease transmission, could be helpful in modeling the spread of epidemics and in assessing containment strategies that rely on travel restrictions.

Acknowledgments

P. C. received financial support from Action Concertée Incentive "Systèmes Complexes en Sciences Humaines et Sociales." The authors thank Dr. Cécile Viboud for interesting suggestions and discussions and for making her data available. M. B. thanks the School of Informatics at Indiana University, where this work was started. Conflict of interest: none declared.

-
- [1] Ferguson NM, Cummings DA, Cauchemez S, et al. Strategies for containing an emerging influenza pandemic in Southeast Asia. *Nature* 2005;437:209-14.
- [2] Longini IM, Nizam A, Xu S, et al. Containing pandemic influenza at the source. *Science* 2005;309:1083-7.
- [3] Ferguson NM, Cummings DA, Fraser C, et al. Strategies for mitigating an influenza pandemic. *Nature* 2006;442:448-52.
- [4] Mills CE, Robins JM, Bergstrom CT, et al. Pandemic influenza: risk of multiple introductions and the need to prepare for them. *PLoS Med* 2006;3:e135. (Electronic article).
- [5] V. Colizza, A. Barrat, M. Barthélemy, A. Vespignani. Modeling the worldwide spread of pandemic influenza. *PLoS Med.* 4, e13 (2007).
- [6] Lloyd-Smith JO, Galvani AP, Getz WM. Curtailing transmission of severe acute respiratory syndrome within a community and its hospital. *Proc Biol Sci* 2003;270:1979-89.
- [7] Lipsitch M, Cohen T, Cooper B, et al. Transmission dynamics and control of severe acute respiratory syndrome. *Science* 2003;300:1966-70.
- [8] Choi BC, Pak AW. A simple approximate mathematical model to predict the number of severe acute respiratory syndrome cases and deaths. *J Epidemiol Community Health* 2003;57:831-5.
- [9] Dye C, Gay N. *Epidemiology*. Modeling the SARS epidemic. *Science* 2003;300:1884-5.
- [10] Donnelly CA, Ghani AC, Leung GM, et al. Epidemiological determinants of spread of causal agent of severe acute respiratory syndrome in Hong Kong. *Lancet* 2003;361:1761-6.
- [11] Wang W, Ruan S. Simulating the SARS outbreak in Beijing with limited data. *J Theor Biol* 2004;227:369-79.
- [12] L. Hufnagel, D. Brockmann, T. Geisel. Forecast and control of epidemics in a globalized world. *Proc. Natl. Acad. Sci. (USA)* **101**, 15124 (2004).
- [13] Meyers LA, Pourbohloul B, Newman ME, et al. Network theory and SARS: predicting outbreak diversity. *J Theor Biol* 2005;232:71-81.
- [14] Colizza V, Barrat A, Barthélemy M, et al. The role of the airline transportation network in the prediction and predictability of global epidemics. *Proc Natl Acad Sci U S A* 2006; 103:2015-20.
- [15] Viboud C, Bjornstad ON, Smith DL, et al. Synchrony, waves, and spatial hierarchies in the spread of influenza. *Science* 2006;312:447-51.
- [16] Brownstein JS, Wolfe CJ, Mandl KD. Empirical evidence for the effect of airline travel on inter-regional influenza spread in the United States. *PLoS Med* 2006;3:e401. (Electronic article).
- [17] Rvachev LA, Longini IM Jr. A mathematical model for the global spread of influenza. *Math Biosci* 1985;75:3-22.
- [18] Flahault A and Valleron AJ. HIV and travel, no rationale for restrictions. *Lancet*. 336, 1197-8 (1990).
- [19] Flahault A, Letrait S, Blin P, et al. Modelling the 1985 influenza epidemic in France. *Stat Med* 1988;7:1147-55.
- [20] World Health Organization. Influenza. Geneva, Switzerland: World Health Organization, 2007. (<http://www.who.int/topics/influenza/en/>). (Accessed January 3, 2007).
- [21] Valleron AJ, Bouvet E, Garnerin P, et al. A computer network for the surveillance of communicable diseases: the French experiment. *Am J Public Health* 1986;76:1289-92.
- [22] Bravata DM, McDonald KM, Smith WM, et al. Systematic review: surveillance systems for early detection of bioterrorism-related diseases. *Ann Intern Med* 2004;140:910-22.
- [23] Centers for Disease Control and Prevention. Flu activity: reports and surveillance methods in the United States. Atlanta, GA: Centers for Disease Control and Prevention, 2007. (<http://www.cdc.gov/flu/weekly/fluactivity.htm>). (Accessed January 3, 2007).

- [24] Bonabeau E, Toubiana L, Flahault A. The geographical spread of influenza. *Proc Biol Sci* 1998;265:2421-5.
- [25] Viboud C, Boelle PY, Pakdaman K, et al. Influenza epidemics in the United States, France, and Australia, 1972–1997. *Emerg Infect Dis* 2004;10:32-9.
- [26] Baroyan OV, Genchikov LA, Rvachev LA, et al. An attempt at large-scale influenza epidemic modeling by means of a computer. *Bull Int Epidemiol Assoc* 1969;18:22-31.
- [27] Anderson RM, May RM. *Infectious diseases of humans: dynamics and control*. New York, NY: Oxford University Press, 1991.
- [28] Greene SK, Ionides EL, Wilson ML. Patterns of influenza-associated mortality among US elderly by geographic region and virus subtype, 1968–1998. *Am J Epidemiol* 2006;163: 316-26.
- [29] Sakai T, Suzuki H, Sasaki A, et al. Geographic and temporal trends in influenzalike illness, Japan, 1992-1999. *Emerg Infect Dis* 2004;10:1822-6.
- [30] Vergu E, Grais RF, Sarter H, et al. Medication sales and syndromic surveillance, France. *Emerg Infect Dis* 2006;12: 416-21.
- [31] Bureau of the Census, US Department of Commerce. *Census 2000 summary file 3*. Washington, DC: Bureau of the Census, 2007. (<http://www.census.gov/population/www/cen2000/>). (Accessed January 8, 2007).
- [32] National Weather Service, National Oceanic and Atmospheric Administration, US Department of Commerce. State data. Silver Spring, MD: National Weather Service, 2007. (<http://www.weather.gov/view/states.php>). (Accessed January 3, 2007).
- [33] Langer WL. The black death. *Sci Am* 1964;210:114-21.
- [34] Noble JV. Geographic and temporal development of plagues. *Nature* 1974;250:726-9.
- [35] Riley S, Ferguson NM. Smallpox transmission and control: spatial dynamics in Great Britain. *Proc Natl Acad Sci U S A* 2006;103:12637-42.

APPENDIX

For all pairs of areas i and j , we compute the usual Pearson correlation coefficient for disease incidence over each epidemic period (composed of n time steps), as

$$r_{ij} = \frac{\sum_{t=1}^n (x_i(t) - \langle x_i \rangle)(x_j(t) - \langle x_j \rangle)}{n S_i S_j}$$

where $x_i(t)$ and $x_j(t)$ are the estimated incidences for areas i and j at time step t , $\langle x_i \rangle$ and $\langle x_j \rangle$ are their averages, and S_i and S_j are their standard deviations.